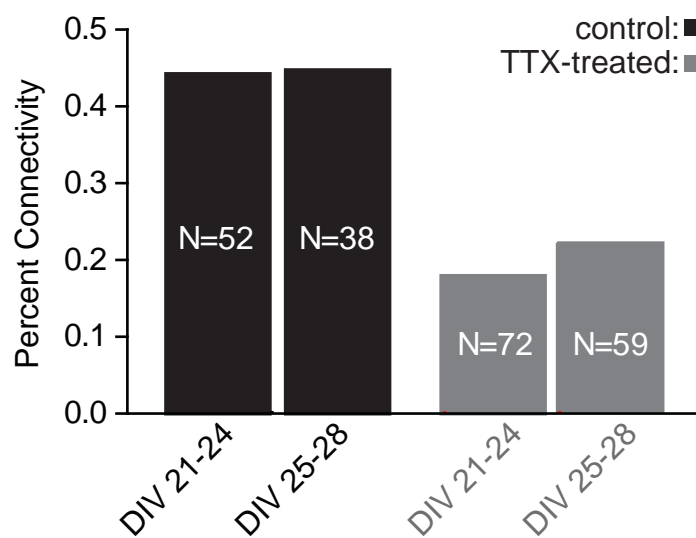
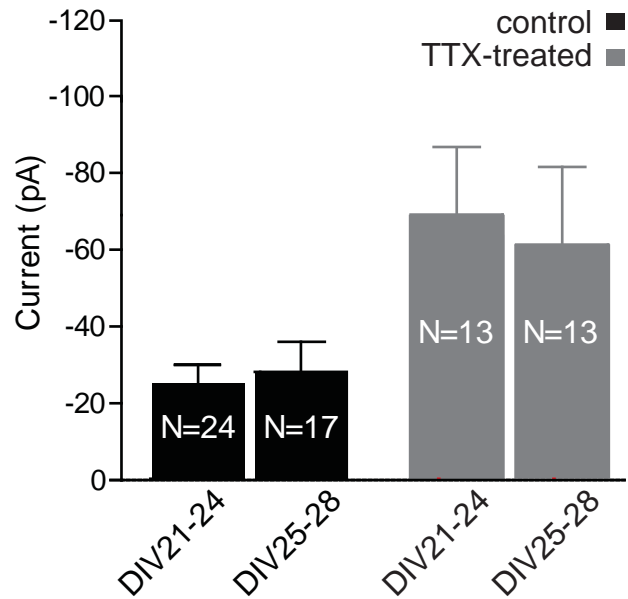


Heterogeneous reallocation of presynaptic efficacy in recurrent excitatory circuits adapting to inactivity

Ananya Mitra, Siddhartha S. Mitra, and Richard W. Tsien

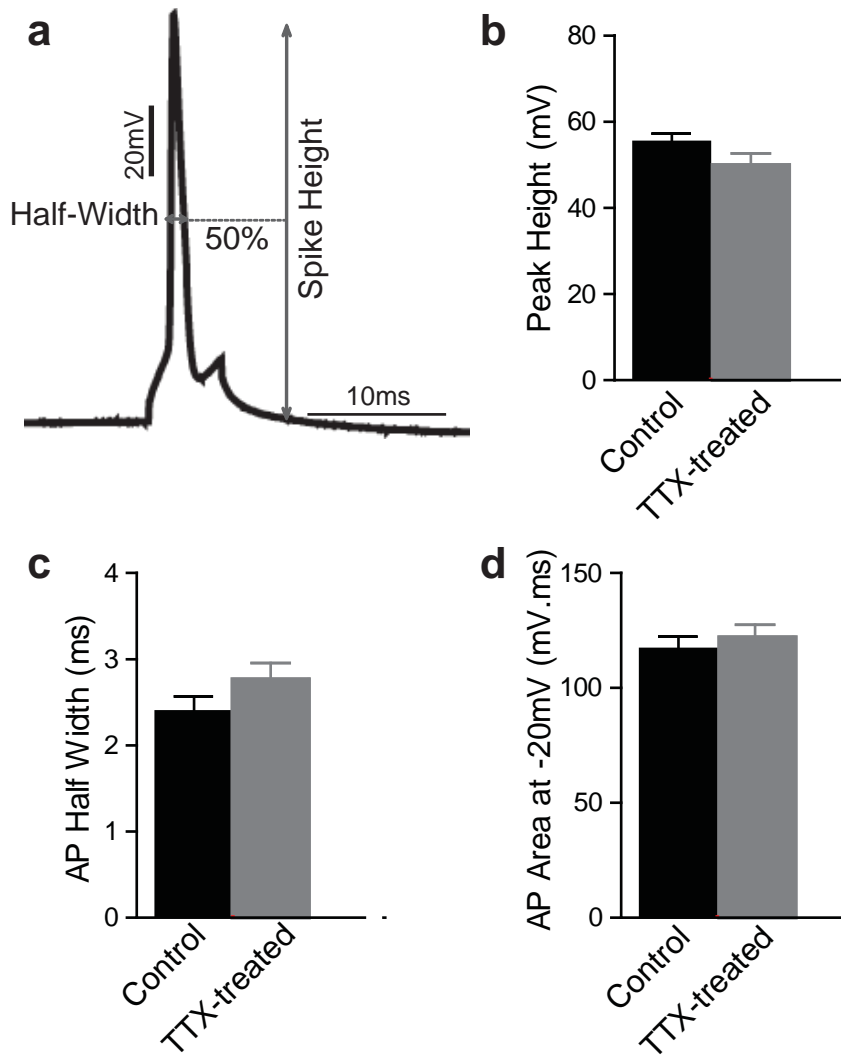
**Supplementary Fig. 1** Dependence of connectivity with age.

To minimize developmental changes that might confound our studies of homeostatic adaptation, we used slices between DIV 21-28 for our experiments. Bar graph shows the percentage connectivity of CA3 pyramids in slices DIV 21-24 and DIV 25-28 in control (46.2% and 44.7% respectively; $P > 0.5$, χ^2 -test; black) and TTX-treated (18.1% and 22.0%; $P > 0.5$, χ^2 -test; gray) conditions.



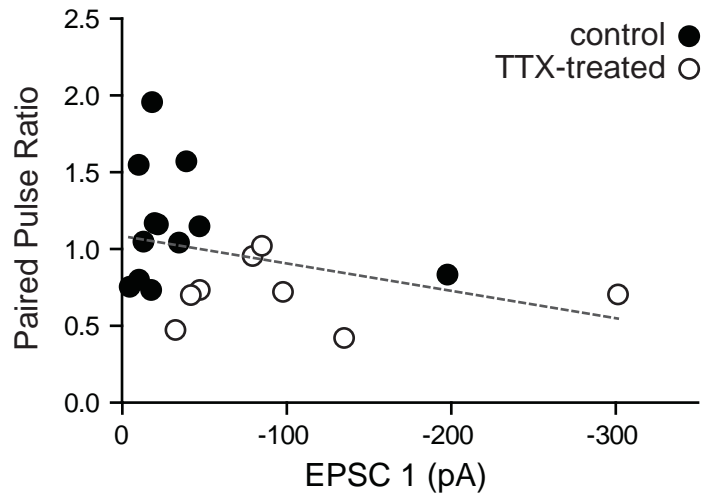
Supplementary Fig. 2 Dependence of synaptic strength with age.

Average evoked EPSC amplitude between connected CA3 pyramidal neurons in slices DIV21-24 and DIV25-28 in control (-25.4±/4.6 pA and -28.2±/7.9 pA respectively; $P > 0.6$, K-S test; black) show no statistical difference in synaptic strength with age. Similar results were found in TTX-treated conditions (-68.6±/17.7 pA and -61.1±/20.7 pA for DIV21-24 and DIV25-28 respectively; $P > 0.5$, K-S test; gray). Error bars represent s.e.m.



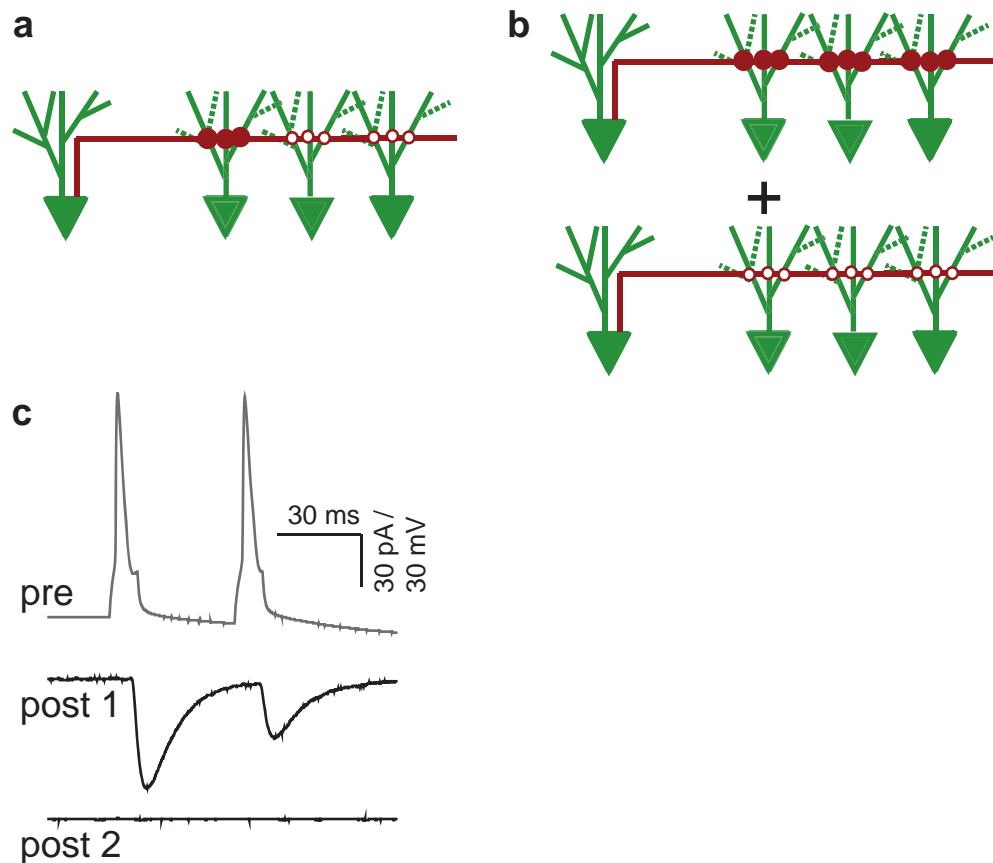
Supplementary Fig 3. Presynaptic action potential parameters.

Action potentials (APs) were generated with brief depolarizing current injections in the presynaptic neuron. (a) Example AP trace from a CA3 neuron in control slice. A comparison of AP characteristics such as spike height (b) and spike shape (half-width (c), spike area (d)) in control (black) and TTX-treated (gray) slices. Error bars represent s.e.m.



Supplementary Fig.4 PPR versus EPSC amplitude.

Each point represents the paired pulse ratio (PPR) plotted against EPSC1 amplitude for each experiment. Linear regression analysis shows no significant difference in the correlation between control (filled circles, N=11) and TTX-treated (empty circles, N=9) pairs ($P > 0.59$). Dashed gray line denotes the negative correlation (slope = 0.0018) between PPR and average EPSC in the pooled data from both groups.



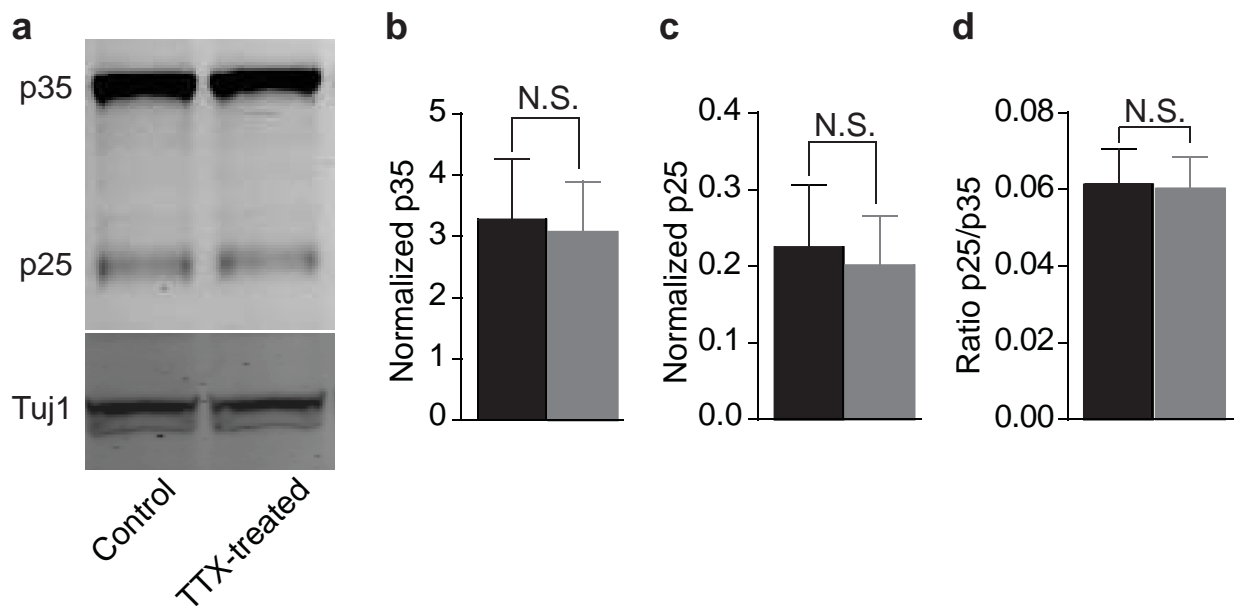
Supplementary Fig. 5 Connectivity determined by concerted versus heterogeneous presynaptic effect.

Schematic representations of two scenarios in activity-deprived slices that could result in decreased functional connectivity. CA3 pyramidal cell body and basal dendrites are in green and axon in red. Filled circles denote active connections and empty circles denote silent synapses.

(a) Disparate postsynaptic targets for a given presynaptic CA3 neuron such that all synapses with some postsynaptic partners are silent (empty circles) while with other postsynaptic partners, all synapses are enhanced (red, filled circles).

(b) An extreme scenario of a concerted presynaptic effect: a drastic shut down at all the boutons (bottom) or an enhancement of presynaptic function of all boutons (top).

(c) Exemplar traces from a triple recording experiment in TTX-treated slices, in which we recorded from three neurons: a single presynaptic cell (grey) and, sequentially, two potential post-synaptic target cells (black). Postsynaptic cell 1 (Post 1) was connected to the presynaptic cell while postsynaptic cell 2 (Post 2) was not, ruling out the extreme scenario depicted in (b).

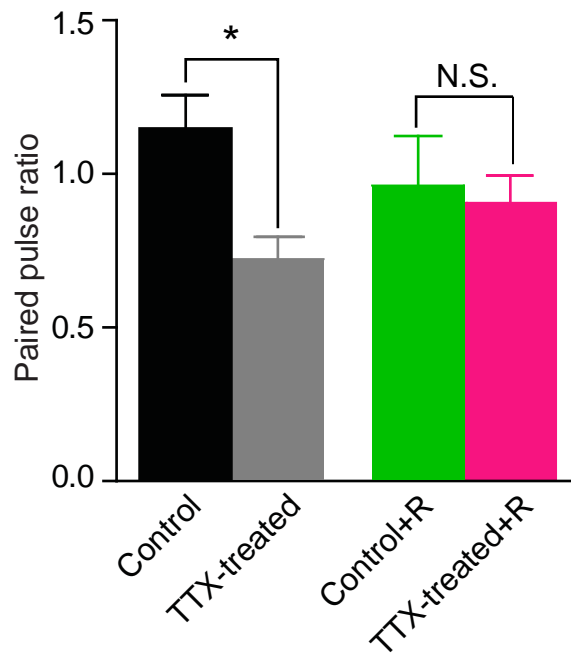


Supplementary Fig.6 Total p35 and 25 protein levels.

(a) Western blot of CA3 tissue lysates in control and TTX-treated slices were immunoblotted with the Anti-p35/p25 and Anti-Tuj1 (normalizing protein). CA3 from slices were micro-dissected from organotypic hippocampal and processed as mentioned in methods. P35, p25 and Tuj1 were immunoblotted using p35/p25-rabbit monoclonal antibody and Tuj1-mouse monoclonal antibody, respectively.

(b-c) Bar graphs showing that total p35 (b) and p25 (c) protein normalized to Tuj1 in control (black) and TTX-treated (gray) slices were similar.

(d) The ratio of p25/p35 is similar in control and TTX-treated slices. A total of 42 slices (n) for each condition were analyzed from 4 different organotypic culture batches (N). Error bars represent s.e.m.



Supplementary Fig. 7 Effect of acute roscovitine on PPR in control and activity-deprived slices.

Graph showing the difference in PPR between CA3 neurons in control (1.15 ± 0.11 , $N=12$, black) and TTX-treated (0.72 ± 0.07 , $N=8$, gray; $P < 0.01$, t test) is abolished in the presence of roscovitine. In the presence of roscovitine, PPR in TTX-treated slices (0.91 ± 0.09 , $N=17$, magenta) was not significantly different from control slices (0.96 ± 0.16 , $N=6$, green; $P > 0.75$, t test).

Supplementary Equation 1. Mathematical Calculation of an Upper Limit on P_r at Synapses between Putatively Unconnected CA3 Neuron Pairs

Here, for the putatively unconnected pairs, we calculate the maximum release probability (P_r) that a single bouton could have and still masquerade as a silent synapse after a long series of trials. The estimate is derived for 30 trials, the minimum used experimentally, although a more stringent upper limit would be derived for the >100 trials in some of the recordings. We consider two scenarios.

(a) the case where the bouton in question is the only anatomically appropriate contributor to the overall connection. Then,

$$\text{Prob(Failure on a single trial)} = (1-P_r)$$

$$\text{Prob(Failure on all 30 trials)} = (1-P_r)^{30}$$

For this to be considered significant, the chances of the null hypothesis being wrong need to be <0.05, or chances of the opposite of the null hypothesis must be >0.95. The null hypothesis is that the synapse is only masquerading as a silent synapse but is really active, and simply appears quiet.

$$\begin{aligned} \text{Then } (1-P_r)^{30} &> 0.95 \\ \Rightarrow (1-P_r) &> (0.95)^{1/30} \\ \Rightarrow P_r &< 1-(0.95)^{1/30} \end{aligned}$$

Thus, $P_r < 0.002$. This upper limit is ~250-fold less than the P_r found for connected pairs.

(b) The case where there are multiple presynaptic boutons that each must fail to release on every trial counted as a failure. If we take into account the finding that roscovitine awakens the connection and makes it behave like a connected pair under control conditions, we can assign the number of boutons per connection as ~13. Then we can substitute $13 \times 30 = 390$ for 30 everywhere 30 appears in the above equation. This puts an even more stringent upper bound on P_r .

In either case, the upper limit on P_r at apparently unconnected synapses is several orders of magnitude lower than in the connected pairs, suggesting an extreme bifurcation in synaptic properties.

Supplementary Equation 2. Modeling Random Assignment of Bouton Properties

We observed 20% connectivity between CA3-CA3 pairs in activity-deprived (TTX-treated) slices. The connectivity was increased to 45% in the presence of roscovitine. Thus,

20/100 connections active after chronic TTX-treatment

45/100 connections active after chronic TTX-treatment + acute roscovitine

$\Rightarrow (45-20)/100 \Rightarrow 25/100$ are “silent” (i.e. can be awakened by acute roscovitine application)

and 55/100 are “anatomically disconnected”

\therefore 20 connections active out of 45 anatomically available connections

$\Rightarrow P_{\text{active}} = 20/45 = 0.444$

where P_{active} = probability of connections being active

If we consider that each connected pair has ~ 13 boutons (N) from mean-variance analysis

$Prob(\text{all boutons silent}) = (1 - P_{\text{active}})^{13} = (0.5556)^{13} = 0.000481$

We can use a χ^2 table to calculate the probability of getting failures at all 13 boutons such that the connection appears “silent” or unconnected

Simple χ^2 table:

	failures	successes
actual	25	20
predicted from random assignment of boutons	$45 \{(0.5556)^{13}\}$ = 0.02	$45 \{1 - (0.5556)^{13}\}$ = 44.98

χ^2 stats =34.0; $P < 0.001$

The above equation calculates the likelihood of random shut down of boutons resulting in a silent or unconnected pair to be *extremely* low ($P < 0.001$). Thus, for a pair of neurons to be assessed as non-connected, all the individual synapses (~ 13) between that pair must be shut down in a cell-wide, all-or none fashion to result in the extreme bifurcation of connectivity that we observe in chronic TTX-treated conditions.